



Boosting Cosmeceutical Peptides: Coupling Imidazolium-Based Ionic Liquids to Pentapeptide-4 Originates New Leads with Antimicrobial and Collagenesis-Inducing Activities

Ana Gomes,^a Lucinda J. Bessa,^{a,b} Iva Fernandes,^a Luísa Aguiar,^a Ricardo Ferraz,^{a,c} Cláudia Monteiro,^{d,e} M. Cristina L. Martins,^{d,e,f} Nuno Mateus,^a Paula Gameiro,^a Cátia Teixeira,^a  Paula Gomes^a

^aLAQV-REQUIMTE, Departamento de Química e Bioquímica, Faculdade de Ciências, Universidade do Porto, Porto, Portugal

^bCentro de Investigação Interdisciplinar Egas Moniz (CiIEM), Egas Moniz - Cooperativa de Ensino Superior, Almada, Portugal

^cCiências Químicas e das Biomoléculas – CISA, Escola Superior de Saúde, Politécnico do Porto, Porto, Portugal

^di3S - Instituto de Investigação e Inovação em Saúde, Universidade do Porto, Porto, Portugal

^eINEB - Instituto de Engenharia Biomédica, Porto, Portugal

^fICBAS, Instituto de Ciências Biomédicas Abel Salazar, Universidade do Porto, Porto, Portugal

ABSTRACT Following our previous reports on dual-action antibacterial and collagenesis-inducing hybrid peptide constructs based on “pentapeptide-4” (PP4, with amino acid sequence KTTKS), whose *N*-palmitoyl derivative is the well-known cosmeceutical ingredient Matrixyl, herein we disclose novel ionic liquid/PP4 conjugates (IL-KTTKS). These conjugates present potent activity against either antibiotic-susceptible strains or multidrug resistant clinical isolates of both Gram-positive and Gram-negative bacterial species belonging to the so-called “ESKAPE” group of pathogens. Noteworthy, their antibacterial activity is preserved in simulated wound fluid, which anticipates an effective action in the setting of a real wound bed. Moreover, their collagenesis-inducing effects *in vitro* are comparable to or stronger than those of Matrixyl. Altogether, IL-KTTKS exert a triple antibacterial, antifungal, and collagenesis-inducing action *in vitro*. These findings provide solid grounds for us to advance IL-KTTKS conjugates as promising leads for future development of topical treatments for complicated skin and soft tissue infections (cSSTI). Further studies are envisaged to incorporate IL-conjugates into suitable nanoformulations, to reduce toxicity and/or improve resistance to proteolytic degradation.

IMPORTANCE As life expectancy increases, diseases causing chronic wound infections become more prevalent. Diabetes, peripheral vascular diseases, and bedridden patients are often associated with non-healing wounds that become infected, resulting in high morbidity and mortality. This is exacerbated by the fact that microbes are becoming increasingly resistant to antibiotics, so efforts must converge toward finding efficient therapeutic alternatives. Recently, our team identified a new type of constructs that combine (i) peptides used in cosmetics to promote collagen formation with (ii) imidazolium-based ionic liquids, which have antimicrobial and skin penetration properties. These constructs have potent wide-spectrum antimicrobial action, including against multidrug-resistant Gram-positive and Gram-negative bacteria, and fungi. Moreover, they can boost collagen formation. Hence, this is an unprecedented class of lead molecules toward development of a new topical medicine for chronically infected wounds.

KEYWORDS antibacterial, antifungal, collagenesis-induction, cosmeceutical peptides, ionic liquid, Matrixyl, antimicrobial activity, collagen boosting, pentapeptide-4

The treatment of complicated skin and soft tissue infections (cSSTI) requires debridement or incision and drainage, complemented with antibiotic therapy. The guidelines for cSSTI treatment recommend the administration of systemic antibiotics that are effective

Editor Amit Singh, Indian Institute of Science Bangalore

Copyright © 2022 Gomes et al. This is an open-access article distributed under the terms of the [Creative Commons Attribution 4.0 International license](https://creativecommons.org/licenses/by/4.0/).

Address correspondence to Paula Gomes, pgomes@fc.up.pt.

The authors declare a conflict of interest. A national patent application protecting peptide-ionic liquid conjugates including those disclosed in this manuscript, for the prevention and/or treatment of skin disorders, has been filed by the following authors: Gomes A, Teixeira C, Bessa L, Fernandes I, Ferraz R, Soares C, Mateus N, Gameiro P, Gomes P (Application No. 118065, filed June 24, 2022).

Received 19 November 2021

Accepted 7 April 2022

Published 11 August 2022

against *methicillin-resistant Staphylococcus aureus* (MRSA) strains, which are among the multidrug-resistant (MDR) pathogens that prevail in health care facilities, followed by an antibiotic therapy program based on the culture assessments for a definitive treatment (1). However, resistance to the available antibiotics is rapidly increasing and currently widespread to many different species of Gram-positive and Gram-negative bacteria. Likewise, fungal infections are becoming more difficult to treat due to the development and spread of resistance among pathogenic fungi.

Peptide-based antimicrobials, like the cyclic lipopeptide daptomycin, offer clinicians an alternative to tackle MDR bacteria in hospital settings, but daptomycin is exclusively active against Gram-positive species, including MRSA (2). However, most cSSTI are of polymicrobial nature, also involving Gram-negative bacteria and fungi, meaning that new options are urgently needed to cope with the emerging post-antibiotic era (3). Fungal colonization of non-healing wounds has been traditionally neglected (4), but Kalan et al. have highlighted the importance of identifying not only bacterial, but also fungal species involved in cSSTI (4), namely, *Cladosporidium* spp. and *Candida* spp., including *C. albicans* and *C. parapsilosis* (5).

The healing process in cSSTI is often delayed or even impaired not only by the microbial infection itself, including biofilm formation in the wound bed, but also by other comorbidities such as diabetes, renal failure, vascular, neuropathic, and genetic disorders, or simply aging (6). In such cases, effective treatment of cSSTI must both quell infection and promote a fast and correct healing. In this regard, collagen, as a structural protein from the extracellular matrix (ECM), plays an important role in key steps of wound healing and closure (7). Because collagen is an endogenous protein, it is regarded as a desirable component for the development of biocompatible and biodegradable wound dressings/biomaterials (8). Along with collagen itself, collagen-derived/inspired peptides, such as cryptic collagen peptides (9), have been also considered as potential promoters of cell migration and proliferation, capable of inducing fibroblasts to produce new collagen, and consequently promoting faster wound healing (10). This motivated the development of the so-called matrikine peptides, and derivatives thereof, for topical application in the treatment of cSSTI, acting by promoting faster wound closure. Matrikine peptides are small peptide fragments that result from proteolysis of ECM macromolecules like collagen or elastin, with diverse potential biomedical applications, including in cosmetics (11, 12). For instance, "pentapeptide-4" (or PP4, with amino acid sequence KTTKS) is a widely studied matrikine that derives from type I human collagen, and is the smallest peptide sequence known to retain a potent ability to stimulate ECM (collagen and fibronectin) production (13, 14). The *N*-palmitoylated form of KTTKS, known as "palmitoyl pentapeptide-4" or Matrixyl, is used in the cosmetics industry due to its ability to cause a skin-rejuvenation/anti-wrinkle effect, probably associated to a collagenesis-inducing action (15, 16).

The potential of PP4 to promote wound healing in the context of cSSTI has recently attracted our attention. Thus, given that this matrikine peptide is devoid of antimicrobial action, we have developed a chimeric peptide where the KTTKS sequence was conjugated to an antimicrobial peptide (AMP), and which displayed potent (i) antibacterial activity against reference and MDR bacteria from clinical isolates; (ii) antibiofilm action; and (iii) a collagenesis-inducing effect comparable to that of Matrixyl (17). Further *N*-terminal modification of the aforementioned chimeric peptide with an imidazolium-based ionic liquid (IL) afforded an equally potent antimicrobial construct with increased stability toward enzyme-mediated modification (18). Indeed, IL are becoming quite attractive for biomedical applications, given their unique physico-chemical characteristics, low cost, and high structural diversity that enables the synthesis of a wide panoply of different IL which can be easily tuned to meet specific requirements, including broad spectrum activity against bacteria (19) and fungi (20). Recently, alkylimidazolium-based IL have been proposed as an alternative antibacterial treatment for cSSTI focusing on Gram-positive pathogens (21). In addition, several IL or alkylimidazolium-derived IL have been found to improve the skin permeation of drugs

(22–24), including ceftazidime, an antibiotic possessing poor water solubility and low skin permeation (25).

In view of the above, we have now investigated if the direct coupling of alkylimidazolium-based IL to the non-antimicrobial KTTKS sequence would afford a new type of peptide-based construct displaying collagenesis-inducing and antimicrobial action, despite not harboring an AMP motif. To this end, three different alkylimidazole-based IL were chemically modified to introduce the alkyne moiety required for subsequent coupling to different azide derivatives of KTTKS. Seven different IL-KTTKS conjugates were produced, and their antibacterial, antifungal, and collagenesis-inducing properties studied, as herein reported and discussed.

RESULTS

Synthesis of the target conjugates. The route toward the target IL-KTTKS conjugates started by the synthesis of the alkyne-modified imidazolium IL (Fig. 1A). Briefly, 1-bromohexadecane and 1-bromotetradecane were first reacted with imidazole, following a procedure previously described by Colonna et al. (step i, Fig. 1A) (26), to afford 1-tetradecyl-imidazole ($C_{14}Im$) and 1-hexadecylimidazole ($C_{16}Im$), respectively. After confirming the structures of both $C_{14}Im$ and $C_{16}Im$ by Nuclear Magnetic Resonance (1H - and ^{13}C -NMR), these imidazoles were reacted with propargyl bromide according to Hu et al. (step ii, Fig. 1A) (27), to afford the three target imidazolium ILs, propargyl-Melm (Pr-Melm), propargyl- $C_{14}Im$ (Pr- $C_{14}Im$) and propargyl- $C_{16}Im$ (Pr- $C_{16}Im$). The structures of these ILs were confirmed by 1H -NMR, ^{13}C -NMR, and electrospray ionization-ion trap mass spectrometry (ESI-IT MS).

In parallel, conveniently modified derivatives of PP4 (amino acid sequence KTTKS) were produced by solid phase peptide synthesis (SPPS), to afford diverse final IL-KTTKS conjugates (Fig. 2) that differed in the: (i) propargyl-imidazolium building blocks used, (ii) insertion site of the latter (*N*-terminus, side chain of either or of both lysine residues), and (iii) length of the spacer between the imidazolium moiety and the peptide's *N*-terminus. To this end, the PP4 sequence was first assembled, according to steps iii and iv in Fig. 1B, and conveniently protected lysine (Fmoc-Lys(Boc)-OH) or azido-lysine (Fmoc-Lys(N_3)-OH) building blocks were inserted in the respective positions of the sequence, according to the desired site for the subsequent introduction of the imidazolium moiety *via* "click" copper (I)-catalyzed alkyne-azide cycloaddition (CuAAC). To produce the peptides modified at the *N*-terminus, the sequence bearing two natural Lys residues was assembled and further elongated through coupling of azido acetic acid (step v, Fig. 1B) yielding a 2-carbon (ethyl) spacer between the *N*-terminal lysine and the imidazolium moiety to be incorporated *via* CuAAC. This click reaction was next performed on-resin on all precursor azido-peptides, using the desired propargyl-imidazolium IL (step vi, Fig. 1B) and CuAAC conditions previously reported by us (18). After acidolytic cleavage (step vii, Fig. 1B) and purification of the crude conjugates thus obtained by reverse-phase preparative high performance liquid chromatography (RP-HPLC), all the resulting IL-KTTKS conjugates were isolated in high purity (>95%), and their expected molecular weights confirmed by ESI-IT MS.

In addition to the target conjugates, the reference cosmeceutical peptide Matrixyl (C_{16} -KTTKS-*OH*), its *C*-terminal carboxamide analogue (C_{16} -KTTKS-*NH*₂), and the native PP4 (KTTKS) were also assembled by SPPS, following procedures recently reported by us (17). For the palmitoylated peptides, after the full amino acid sequence of PP4 was assembled, palmitic acid (C_{16}) was coupled. Then, acidolytic cleavage from the solid support delivered the crude peptides that were purified by RP-HPLC. The final peptides were obtained in high purity and their molecular weights confirmed by ESI-IT MS.

Antibacterial activity *in vitro*. The antimicrobial activity of the IL-KTTKS conjugates was assessed *in vitro* against reference bacterial strains (American Type Culture Collection, ATCC). The minimal inhibitory concentration (MIC) was determined according to the Clinical and Laboratory Standards Institute (CLSI) guidelines (28) against Gram-positive (*S. aureus*, *Enterococcus faecalis*) and Gram-negative (*Escherichia coli*, *Pseudomonas aeruginosa*) bacteria. The MIC values obtained are shown in Table 1. Notably, the reference peptides C_{16} -KTTKS-*NH*₂ and C_{16} -KTTKS-*OH* were respectively soluble in water and dimethyl sulfoxide

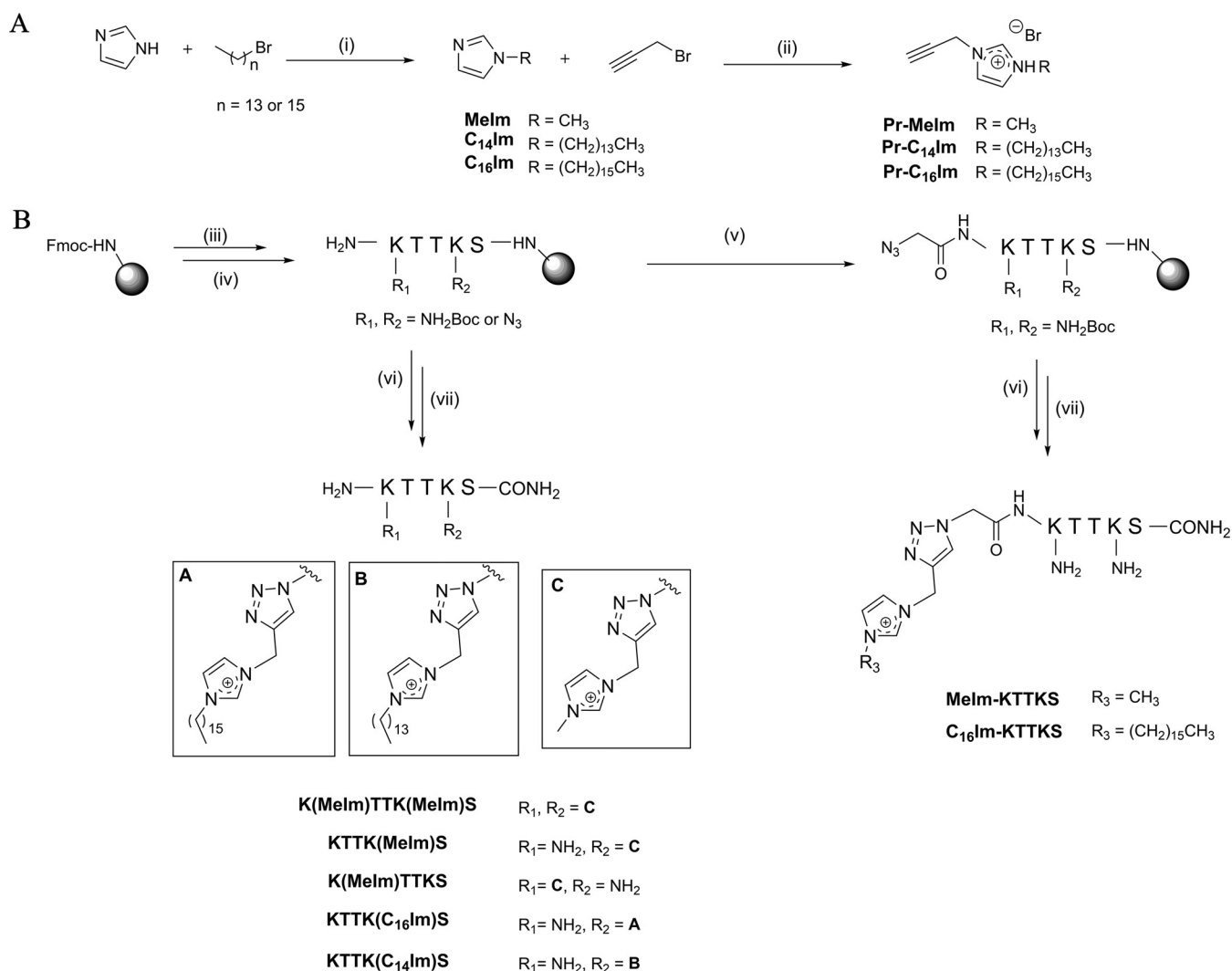


FIG 1 Route to the target IL-KTTKS conjugates. (A) Synthesis of the alkyne derivatives of the IL: (i) 1 molar equivalent (eq) of imidazole, 1.5 eq of potassium hydroxide, 1-bromotetradecane or 1-bromohexadecane in dimethyl sulfoxide (DMSO), 70°C, 5 h; (ii) 1.1 eq of C₆Im, C₁₄Im or Melm and 1.0 eq of propargyl bromide (80% in toluene), 40°C, 24 h. (B) Synthesis of the azide derivatives of KTTKS and their coupling to the alkyne-IL *via* CuAAC: (iii) 5 eq of Fmoc-protected amino acid, 10 eq of *N*-ethyl-*N,N*-diisopropylamine (DIEA) and 5 eq of *O*-(benzotriazol-1-yl)-*N,N,N',N'*-tetramethyluronium hexafluorophosphate (HBTU) in *N,N*-dimethylformamide (DMF), 1 h, room temperature (r.t.); (iv) 20% piperidine in DMF, 15 min, r.t.; (v) 5 eq of azido acetic, 10 eq of DIEA, 5 eq of HBTU, 1 h, r.t.; (vi) 10 eq of DIEA, 10 eq of 2,6-lutidine, 1 eq of copper(I) bromide, 1 eq of sodium *L*-ascorbate and 1 eq of either Pr-Melm, Pr-C₁₆Im, or Pr-C₁₄Im, in DMF:acetonitrile (ACN) (3:1 vol/vol), 24 h, r.t.; (vii) trifluoroacetic acid (TFA)/triisopropylsilane (TIS)/distilled water (95:25:2.5 vol/vol/vol).

(DMSO), but both precipitated when diluted in cation-adjusted Mueller-Hinton broth (MHB2), the culture medium recommended by the CLSI guidelines, which hampered the determination of the MIC values for these reference peptides. Data in Table 1 show, as expected, that the peptide KTTKS alone is devoid of significant antibacterial activity, and that MIC values for the reference 1-hexadecyl-3-methylimidazolium bromide ([C₁₆ M1Im] [Br]) IL are in agreement with those previously reported (29). Interestingly, all conjugates bearing methyl imidazolium (Melm) units were inactive against the tested bacterial species, even at the highest concentrations used, regardless the number or position of the Melm moieties in the overall structure. In turn, replacing the methyl substituent in the imidazolium ring by either a tetradecyl (C₁₄) or a hexadecyl (C₁₆) group, led to an improvement in the antibacterial activity, delivering MIC values from 6.45 to 52.6 μg/mL, hence adding antimicrobial activity to the parent KTTKS peptide. Given that KTTK(C₁₆Im)S and C₁₆Im-KTTKS showed the strongest antibacterial activities, and reflect two different conjugation

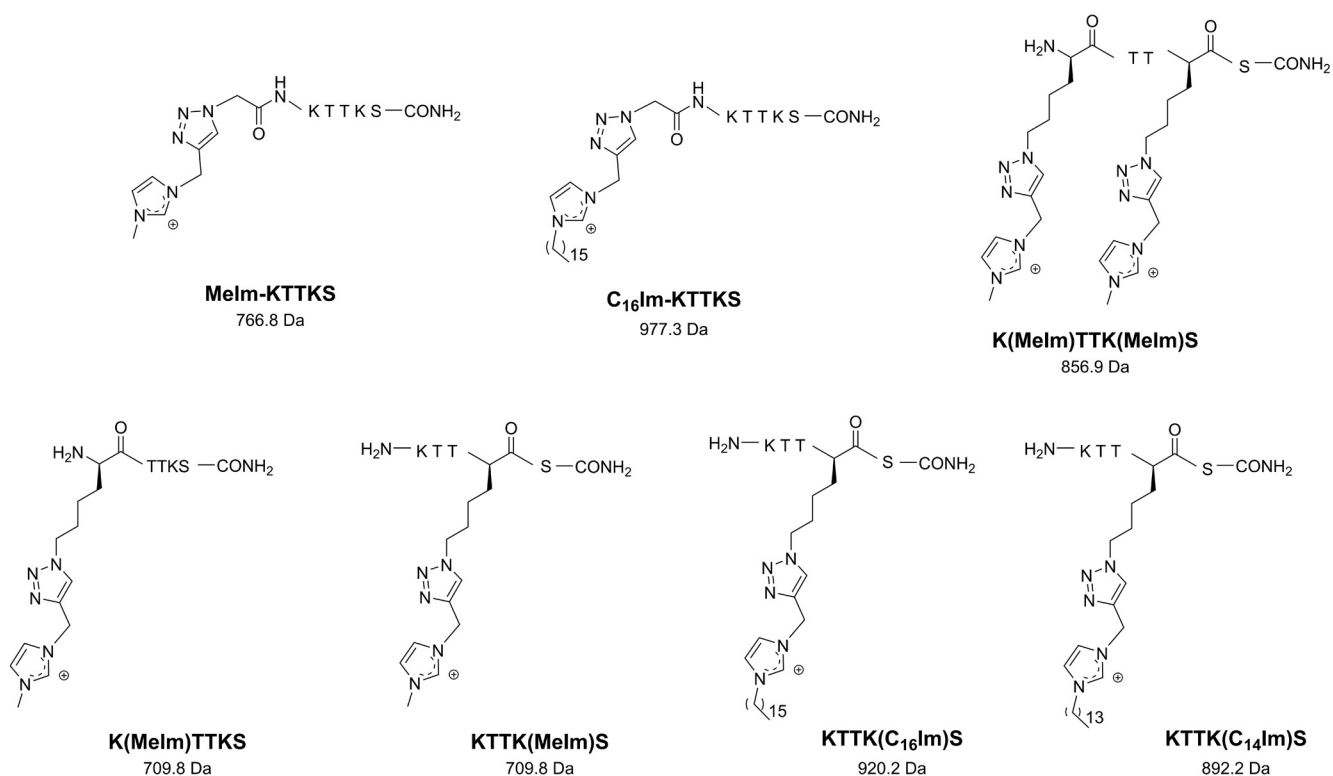


FIG 2 Structure of IL-KTTKS conjugates and corresponding molecular weight (in Da). The amino acids are represented in single letter code as defined by the IUPAC-IUBMB guidelines on nomenclature and symbolism for amino acids and peptides; exception is made to the amino acid residues whose side chain was coupled to ionic liquids *via* click chemistry, in which case the full modified structure is shown.

positions, both these peptides were further investigated by determining their MIC against *Staphylococcus epidermidis*, *Streptococcus pyogenes* (both Gram-positive), and *Klebsiella pneumoniae* (Gram-negative), chosen due to their abundance in the skin (*S. epidermidis*) (30), relevance to cSSTI (*S. pyogenes*) (31–33), and relation to the so-called “ESKAPE” pathogens (*K. pneumoniae*) (34). The noncovalent mixture of the parent peptide KTTKS and the [C₁₆ M1Im][Br] ionic liquid, presented MIC values comparable to those of [C₁₆ M1Im][Br] alone.

The antibacterial activities of the best couple of conjugates, i.e., C₁₆Im-KTTKS and KTTK (C₁₆Im)S, and of the reference antibiotic ciprofloxacin, were further assessed against MDR

TABLE 1 MIC values ($n = 3$) in μM (in $\mu\text{g}/\text{mL}$) of the IL-KTTKS conjugates against Gram-negative and Gram-positive bacteria (ATCC reference strains)

Peptide	MIC in μM (in $\mu\text{g}/\text{mL}$)						
	<i>E. coli</i> ATCC 25922	<i>P. aeruginosa</i> ATCC 27853	<i>S. aureus</i> ATCC 29213	<i>E. faecalis</i> ATCC 29212	<i>K. pneumoniae</i> ATCC 138830	<i>S. epidermidis</i> ATCC 14990	<i>S. pyogenes</i> ATCC 19615
K(Melm)TTKS	> 1030.1 (731.2)				ND ^a	ND ^a	ND ^a
KTTK(Melm)S	> 954.2 (677.3)				ND ^a	ND ^a	ND ^a
K(Melm)TTK(Melm)S	> 1245.5 (1067.4)				ND ^a	ND ^a	ND ^a
KTTK(C ₁₄ Im)S	29.5 (26.3)	58.9 (52.6) ^b	29.5 (26.3)	58.9 (52.6) ^b	ND ^a	ND ^a	ND ^a
KTTK(C ₁₆ Im)S	7.0 (6.45)	32.5 (29.9)	14.0 (12.9)	32.5 (29.9)	53.8 (49.5)	5.4 (5.0)	10.9 (10.0)
Melm-KTTKS	> 825.9 (633.4)				ND ^a	ND ^a	ND ^a
C ₁₆ Im-KTTKS	14.3 (14.0)	28.7 (28.0)	14.3 (14.0)	28.7 (28.0)	27.4 (26.8)	9.5 (9.3)	18.9 (18.5)
KTTKS	> 1820 ^c				ND ^a	ND ^a	ND ^a
[C ₁₆ M1Im][Br]	60	> 240	0.94 ^d	0.94 ^c	60	ND ^a	ND ^a
KTTKS:[C ₁₆ M1Im][Br] (1:1)	60	> 240	0.94 ^d	0.18 ^c	60	ND ^a	ND ^a
Ciprofloxacin	0.012 (0.004)	0.18 (0.06)	1.5 (0.5)	0.38 (0.125)	0.75 (0.25)	0.75 (0.25)	6.04 (2.0)

^aNot determined.

^bThe minimal bactericidal concentration (MBC) was 2× the MIC.

^cMBC = 15 μM .

^dMBC = 30 μM ; in all other cases, the MBC was equal to the MIC.

^eValue from (17).

TABLE 2 MIC values ($n = 3$) in μM (in $\mu\text{g}/\text{mL}$) for $\text{C}_{16}\text{Im-KTTKS}$ and $\text{KTTK}(\text{C}_{16}\text{Im})\text{S}$ against MDR clinical isolates of Gram-positive and Gram-negative bacteria

MDR	Peptide		Ciprofloxacin
	$\text{C}_{16}\text{Im-KTTKS}$	$\text{KTTK}(\text{C}_{16}\text{Im})\text{S}$	
KP010	37.9 (37.0)	21.7 (20.0)	48.0 (16.0)
PA004	18.9 (18.5)		96.0 (32.0)
SA007	18.9 (18.5) ^a		193.0 (64.0)

^aThe MBC was $2\times$ the MIC; In all other cases the MBC was equal to the MIC.

clinical isolates of *K. pneumoniae* (KP010), *S. aureus* (SA007), and *P. aeruginosa* (PA004). MIC values thus obtained are displayed in Table 2 and show that both conjugates preserve their antibacterial activity observed against susceptible ATCC bacterial strains. Relevantly, the conjugates were clearly more active than the reference antibiotic ciprofloxacin against the MDR isolates; for instance, the MIC value obtained for $\text{C}_{16}\text{Im-KTTKS}$ against SA007 is nearly 10-fold higher than that of ciprofloxacin.

The antibacterial activity of $\text{C}_{16}\text{Im-KTTKS}$ and $\text{KTTK}(\text{C}_{16}\text{Im})\text{S}$ was also assessed in simulated wound fluid (SWF) (35) against *S. aureus* (ATCC 29213), to check if it was preserved in this medium. MIC values were obtained in both SWF and MHB media in three independent experiments run in triplicates (Table 3), and indicated that the antibacterial activity in SWF was the same as that in MHB for $\text{C}_{16}\text{Im-KTTKS}$, and decreased for $\text{KTTK}(\text{C}_{16}\text{Im})\text{S}$ displaying a MIC twice as high.

Antifungal activity in vitro. The antifungal activity of the best couple of IL-KTTKS conjugates, their parent building blocks, and respective noncovalent 1:1 mixture, were all assessed against three species of *Candida*, namely, *Candida albicans* (ATCC 90028), *Candida glabrata* (ATCC 90030), and *Candida parapsilosis* (ATCC 22019). The MIC values were determined according to the European Committee on Antimicrobial Susceptibility Testing (EUCAST) protocol (36) and are shown on Table 4. Both conjugates, $\text{KTTK}(\text{C}_{16}\text{Im})\text{S}$ and $\text{C}_{16}\text{Im-KTTKS}$, were equally active against all *Candida* spp, with MIC values ranging from 2.4 to 5.4 μM . Both peptides were twice more active against *C. parapsilosis* than against the other two *Candida* species. Relevantly, the noncovalent mixture $\text{KTTKS}:[\text{C}_{16}\text{M1Im}][\text{Br}]$ (1:1) showed a potent activity against all *Candida* spp, being equipotent to the parent IL alone, and both seven times more active than the reference antifungal drug fluconazole.

Toxicity to HFF-1 and HaCaT cells. The cytotoxicity of $\text{KTTK}(\text{C}_{16}\text{Im})\text{S}$ and $\text{C}_{16}\text{Im-KTTKS}$ conjugates was assessed on human foreskin fibroblasts (HFF-1) and human immortalized keratinocytes (HaCaT). The results shown in Table 5, are expressed as the conjugate concentration causing a 50% cell growth inhibition (IC_{50}). As expected from previous reports (37), both the parent peptide sequence KTTKS and the derived reference cosmeceutical Matrixyl ($\text{C}_{16}\text{-KTTKS-OH}$) did not show relevant toxicity against the cell lines tested, at up to 100 μM . In turn, the parent IL $[\text{C}_{16}\text{M1Im}][\text{Br}]$ and its covalent equimolar mixture with PP4, $\text{KTTKS}:[\text{C}_{16}\text{M1Im}][\text{Br}]$ (1:1), were significantly toxic. Interestingly, covalent conjugation of the peptide to the IL resulted in an intermediate situation, as conjugates were more toxic than the peptide alone, but clearly less toxic than the IL alone or than its noncovalent mixture with the peptide.

Collagen production in vitro. The point of conjugating antimicrobial ILs to a collagenesis-inducing peptide was to afford a simple construct able to exert a dual anti-

TABLE 3 MIC (MBC) values ($n = 3$) in $\mu\text{g}/\text{mL}$ for $\text{C}_{16}\text{Im-KTTKS}$ and $\text{KTTK}(\text{C}_{16}\text{Im})\text{S}$ against *S. aureus* (ATCC 29213) in MHB and SWF

Peptide	MIC in $\mu\text{g}/\text{mL}$ [MBC]	
	MHB	SWF
$\text{C}_{16}\text{Im-KTTKS}$	16-32 [32 to 64]	16-32 [32 to >64]
$\text{KTTK}(\text{C}_{16}\text{Im})\text{S}$	32 [64 to 128]	64-128 [128 to >128]

TABLE 4 MIC values ($n = 2$) in μM (in $\mu\text{g/mL}$) for the best performing conjugates, their parent building blocks, and respective 1:1 noncovalent mixture on ATCC *Candida* spp.

Peptide	MIC in μM (in $\mu\text{g/mL}$)		
	<i>C. albicans</i> ATCC 90028	<i>C. glabrata</i> ATCC 90030	<i>C. parapsilosis</i> ATCC 22019
KTTK(C ₁₆ m)S	5.4 (5.0)	5.4 (5.0)	2.7 (2.5)
C ₁₆ Im-KTTKS	4.7 (4.6)	4.7 (4.6)	2.4 (2.3)
KTTKS	>60	>60	>60
[C ₁₆ M1Im][Br]	0.93	0.93	0.93
KTTKS:[C ₁₆ M1Im][Br] (1:1)	0.93	0.93	0.93
Fluconazole	1.6 (0.5)	26 (8)	6.5 (2)

crobal and skin rebuilding action. Therefore, the two best IL-KTTKS conjugates were further tested for their ability to promote collagen production by human dermal fibroblasts (HDF) *in vitro*. This was assessed using the Sircol kit assay, whereby the amount of newly formed collagen in the ECM that is deposited in the microwell-plated cell cultures is solubilized in an acidic medium and next quantified through a collagen standard curve according to the Sircol kit assay procedure (38). Assays were conducted in different conditions for comparison, namely, in the presence of the reference cosmeceutical Matrixyl (positive control – C₁₆-KTTKS-OH), of the test conjugates KTTK(C₁₆Im)S and C₁₆Im-KTTKS, and in the absence of any peptide (negative control). Data presented in Fig. 3 show that both conjugates induce HDF cells to produce more collagen, compared to the negative control. No significant difference was observed between both conjugates or between KTTK(C₁₆Im)S conjugate and reference Matrixyl, demonstrating that the ability of Matrixyl to induce collagenesis is not affected by the introduction of the imidazolium IL at the Lys side chain of the peptide sequence.

DISCUSSION

Recently, we have demonstrated that it is possible to produce a dual-action antimicrobial and collagenesis-inducing chimeric peptide, by combining the amino acid sequence of an AMP to that of the non-antimicrobial well-known cosmeceutical peptide PP4 (17). We were further able to show that such potent antimicrobial activity was preserved when coupling an imidazolium IL to the *N*-terminus of the chimeric peptide *via* the CuAAC “click” approach, which conferred the peptide resistance to enzyme-mediated modification (18). Based on these findings, and on the widely reported antimicrobial properties of imidazolium (and other) ILs (21, 39, 40), we hypothesized that it might be possible to preserve the dual antimicrobial and collagenesis-inducing activity by leaving the AMP sequence out and coupling the IL directly to the amino acid sequence of the cosmeceutical peptide PP4. The antibacterial activity of the new constructs herein presented, IL-KKTKS, was assessed against reference bacterial strains and results obtained allow us to advance a couple of structure-activity relationships (SAR) on the (i) IL insertion site, as the covalent graft was at either the *N*-terminus or the Lys1/Lys4 side chains of the KTTKS sequence, and (ii) length of

TABLE 5 IC₅₀ values, in μM , obtained for the best performing conjugates, their parent building blocks, and respective noncovalent 1:1 mixture, against HFF-1 and HaCaT cells (after 24 h of incubation)

Peptide	IC ₅₀ \pm SEM (μM) ^a	
	HaCaT	HFF-1
KTTK(C ₁₆ Im)S	23.05 \pm 1.10	12.71 \pm 1.06
C ₁₆ Im-KTTKS	36.60 \pm 1.09	22.46 \pm 1.08
C ₁₆ -KTTKS-OH	>100	79.74 \pm 2.82
KTTKS	>100	ND
[C ₁₆ M1Im][Br]	6.27 \pm 1.02	ND
KTTKS:[C ₁₆ M1Im][Br] (1:1)	6.46 \pm 1.01	8.47 \pm 1.03

^aData expressed as mean \pm SEM of 2 independent experiments ($n = 8$).

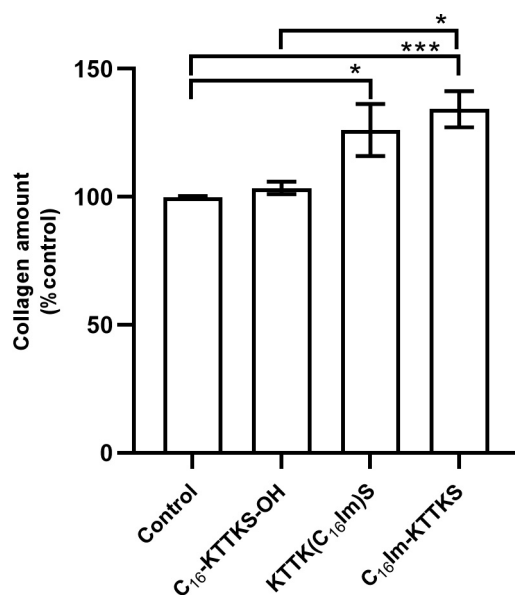


FIG 3 Collagen synthesis by HDF, in the presence of C₁₆-KTTKS-OH (Matrixyl), KTTK(C₁₆Im)S and C₁₆Im-KTTKS at 5 μM, using the Sircol Kit. Data are presented as mean ± SEM (three independent experiments in triplicates) expressed in collagen amount (% of control); *, $P < 0.05$; **, $P < 0.01$.

the alkyl substituent in the imidazole ring, which was varied between one (methyl or Me spacer), 14 (tetradecyl or C₁₄ spacer), and 16 (hexadecyl or C₁₆ spacer) carbons. Hence, antibacterial activity (i) increases with the length of the alkyl substituents in the IL moiety [KTTK(C₁₄Im)S versus KTTK(C₁₆Im)S] and (ii) is depleted in all conjugates bearing the methyl-substituted imidazolium IL, regardless of other structural features. This alkyl chain length effect agrees with previous studies on antimicrobial ILs (29, 41). Moreover, MIC values were also determined for the parent building blocks KTTKS and [C₁₆ M1Im][Br], as well as for their noncovalent equimolar mixture, indicated as KTTKS:[C₁₆ M1Im][Br] (1:1), so that the importance of covalent conjugation could be assessed. The noncovalent mixture KTTKS:[C₁₆ M1Im][Br] (1:1) presented MIC values similar to those of [C₁₆ M1Im][Br] alone, confirming that the IL building block is mainly responsible for the activity observed for the mixture, as expected. Interestingly, when comparing the MIC values of the noncovalent mixture KTTKS:[C₁₆ M1Im][Br] (1:1) with those of the covalent conjugates KTTK(C₁₆Im)S and C₁₆Im-KTTKS, it is apparent that covalent conjugation is clearly beneficial for activity against Gram-negative bacteria, but not so much against Gram-positive bacteria. Still, whereas the noncovalent mixture is bacteriostatic for Gram-positive species at MIC values, the covalent conjugates are bactericidal at these concentrations. These results indicate that the antibacterial activity of the covalent conjugates KTTK(C₁₆Im)S and C₁₆Im-KTTKS is not only modulated by the IL building block, but also by its conjugation to the peptide, eventually due to the CuAAC-mediated insertion of the 1,2,3-triazole ring that has been proven as an important antimicrobial pharmacophore (42). Hence, biophysical studies should be performed to further explore the mechanism(s) of action of IL-KTTKS conjugates. The conjugates KTTK(C₁₆Im)S and C₁₆Im-KTTKS also showed a potent activity against MDR clinical isolates of Gram-positive and Gram-negative bacteria, being more active than the reference antibiotic ciprofloxacin. This is a relevant finding, considering that the three clinical isolates tested refer to bacterial species belonging to the “ESKAPE” group of pathogens which encompasses life-threatening nosocomial pathogens, namely, *Enterococcus faecium*, *Staphylococcus aureus*, *Klebsiella pneumoniae*, *Acinetobacter baumannii*, *Pseudomonas aeruginosa*, and *Enterobacter* spp. The ability of “ESKAPE” pathogens to escape the action of currently available antibiotics is one of the major health care threats of our times, especially for Gram-negative bacteria, against which the world is running out of effective options (43). Additionally, the conjugates showed to retain

(C₁₆Im-KTTKS) or slightly decrease (KTTK(C₁₆Im)S) the antibacterial activity against *S. aureus* in SWF. The real wound fluids contain proteins, including growth factors and proteases, among other constituents, with a specific composition that depends on if it is a healing or a non-healing wound. In fact, the fluid formed in the open wound generally has wound-healing properties and is beneficial for a fast wound recovery, however in the presence of a high amount of certain components or of microorganisms, the healing process can be delayed or impaired (44). Moreover, the presence of metalloproteinases and other enzymes may rapidly inactivate any peptide-based wound treatments. As such, these preliminary observations using SWF, which mimics the wound exudate, are relevant as they are indicative that the IL-peptide conjugates, especially C₁₆Im-KTTKS, can be more stable in the wound environment compared with analogues where the peptide is not protected at the *N*-terminus, which is in line with our previous observations regarding the stabilization effect of linking an ionic liquid to the *N*-terminus of a bioactive peptide (18).

The IL-KTTKS conjugates herein advanced have also shown interesting antifungal properties, especially against *C. parapsilosis*. This is one of the most common non-*C. albicans* species of *Candida*, which are regarded as important nosocomial pathogens of concern as they were reported to be involved in cases of sepsis (45) and cSSTI (5). In this regard, the antifungal activity of the conjugates was assessed, and MIC values observed were as low as 2.4 and 2.7 μ M against *C. parapsilosis* and 4.7 and 5.7 μ M against *C. albicans*. This concurs with recent findings by Reddy et al., showing that imidazolium ILs with long alkyl chains, e.g., dodecyl and hexadecyl, have potent activity against *C. albicans* (20). Still, as observed in antibacterial activity assays, the non-covalent mixture and the parent IL are more potent than the IL-KTTKS conjugates against *Candida* spp., which indicates that the antifungal activity of the covalent conjugates is not only modulated by the IL building block, but also by their conjugation to the peptide (devoid of antifungal activity). Therefore, further biophysical studies should be performed to shed some light into possible mechanism(s) of action of IL-KTTKS conjugates against *Candida* species.

The evaluation of the cytotoxicity of the IL-KTTKS conjugates is obviously important on its own to check for selectivity, but also due to the toxicity effects often associated to IL, depending on, e.g., cation alkyl chain length (46) or specific ions used (47). The parent IL [C₁₆ M1Im][Br] and its covalent equimolar mixture with the peptide, KTTKS:[C₁₆ M1Im][Br] (1:1), were significantly toxic against the human cell lines tested, in agreement with previous reports on ILs (19). Therefore, covalent conjugation of the IL to the peptide confers on the one hand, antimicrobial activity to an otherwise peptide building block devoid of such activity and, on the other, reduced cytotoxicity compared to the parent IL.

The conjugates C₁₆Im-KTTKS and KTTK(C₁₆Im)S were further assessed for their ability to induce collagen production by HDF *in vitro*. The conjugates showed to be comparable to the reference cosmeceutical Matrixyl and more active than the control. The mechanism behind the collagen inducing effect of Matrixyl is not well explored, although Jones et al. have suggested that the self-assembling properties of the Matrixyl amphiphilic structure favors recognition of pro-collagen residues, *via* formation of nanotapes that expose relevant peptide epitopes (48). Irrespective of that, no significant difference between both conjugates were observed, indicating that changing the side chain of Lys4 did not affect the peptide's collagenesis-inducing behavior.

Altogether, our findings are unprecedented as well as remarkable, as they provide confirmation of our initial hypothesis, by advancing a couple of IL-peptide conjugates, C₁₆Im-KTTKS and KTTK(C₁₆Im)S, that possess antibacterial, antifungal, and collagenesis-inducing activity *in vitro*, the latter being actually comparable with that of the cosmeceutical ingredient Matrixyl based on the KTTKS peptide. Further, the site of insertion of the IL does not significantly affect the overall *in vitro* properties of the conjugates [C₁₆Im-KTTKS *versus* KTTK(C₁₆Im)S], although *N*-terminal conjugation seems to better preserve the conjugates' antibacterial action in SWF and to improve the collagen synthesis by HDF. However, further studies are envisaged to incorporate IL-conjugates into nanoformulations, which will reduce toxicity and/or improve resistance to proteolytic degradation. Moreover, because

the IL-KTKS conjugates will be applied in the treatment of cSSTI, which are mainly polymicrobial infections, the antimicrobial activity of IL-KTKS on polymicrobial cultures will be further investigated. This will enable selection of best IL-KTKS based formulations to advance for *in vivo* studies.

Considering that the KTKS and other small collagenesis-boosting peptides are already produced at industrial scale as ingredients for cosmetic products, this report unveils the value of IL-cosmeceutical peptide conjugates as a promising start for future development of cost-effective topical formulations for the treatment of skin disorders, from mild to severe ones like cSSTI.

MATERIALS AND METHODS

Chemical synthesis. (i) 1-tetradecylimidazole (C₁₄-Im) and 1-hexadecylimidazole (C₁₆-Im). Imidazole (0.5 g; 7.3 mmol; 1 eq; Sigma-Aldrich) and potassium hydroxide (0.62 g, 11.0 mmol, 1.5 eq) were added to a round-bottom flask and dissolved in DMSO (12 mL; MERCK). The reaction mixture was left at 70°C under magnetic stirring for 30 min, after which either 1-bromotetradecane (2.18 mL; 7.3 mmol; 1.0 eq; Sigma-Aldrich) or 1-bromohexadecane (2.26 mL, 7.3 mmol, 1.0 eq; Sigma-Aldrich) was slowly added. The reaction was allowed to proceed under magnetic stirring at 70°C for 5 h, then the mixture was cooled down to room temperature (r.t.), and water (30 mL) was added. After placing this mixture in an ice bath, a white solid was formed and next filtered, washed with water (3 × 250 mL), and dried under vacuum overnight to afford the final 1-alkylimidazoles in 88% (C₁₄-Im) and 84% (C₁₆-Im) yield. The structures of these final compounds were confirmed by ¹H-NMR and ¹³C-NMR, according with the spectral data below. The multiplicity of ¹H-NMR signals is given as: s, singlet; d, doublet; t, triplet; m, unresolved multiplet; q, quintuplet.

(a) *1-tetradecyl-imidazole*. Yellow oil (1.71 g, 88%); δ_H/ppm (400 MHz, CDCl₃) 7.46 (s, 1H), 7.02 (s, 1H), 6.90 (s, 1H), 3.89 (t, 2H, J = 7.6 Hz), 1.73 (q, 2H, J = 7.0 Hz), 1.27-1.22 (m, 22H), 0.85 (t, 3H, J = 6.9 Hz); δ_C/ppm (100 MHz, CDCl₃) 137.1, 129.2, 118.8, 47.2, 32.0, 31.1, 29.7-29.4, 26.6, 22.7, 14.2;

(b) *1-hexadecylimidazole*. White solid (1.81 g, 84%); δ_H/ppm (400 MHz, CDCl₃) 7.57 (s, 1H), 7.06 (s, 1H), 6.90 (s, 1H), 3.93 (t, 2H, J = 7.1 Hz), 3.53 (q, 2H, J = 7.1 Hz), 1.29-1.24 (m, 26H), 0.87 (t, 3H, J = 6.9 Hz); δ_C/ppm (100 MHz, CDCl₃) 137.0; 128.8; 119.0; 47.4; 32.0; 31.1; 29.8-29.1; 26.6; 22.8; 14.2;

(ii) 1-methyl-3-(prop-2-enyl)imidazolium bromide (Pr-Melm), 1-tetradecyl-3-(prop-2-enyl)imidazolium bromide (Pr-C₁₄Im), and 1-hexadecyl-3-(prop-2-enyl)imidazolium bromide (Pr-C₁₆Im). An 80% solution of propargyl bromide in toluene (250 μL; 2.24 mmol, 1.0 eq; Fluorochem) was slowly added to a round-bottom flask containing 1-methyl-imidazole (Alfa Aesar; 195 μL, 2.5 mmol, 1.1 eq), 1-tetradecyl-imidazole (0.664 g, 2.5 mmol, 1.1 eq) or 1-hexadecylimidazole (0.723 g, 2.5 mmol, 1.1 eq), and the mixture kept under magnetic stirring at 40°C for 24 h. After cooling down the yellow oily mixture formed to r.t., dichloromethane (DCM, 4 mL; CARLO ERBA) was added, followed by addition of cold diethyl ether (10 mL; Fisher Chemical). The suspension was placed in an ice bath, occurring precipitation of a white solid that was filtered and washed with diethyl ether (10 mL). This solid was re-dissolved and re-precipitated three times upon alternate addition of 5-mL portions of DCM and 10-mL portions of diethyl ether, to afford the final products in 77% (Pr-Melm), 45% (Pr-C₁₄Im) and 97% (Pr-C₁₆Im) yields. The structures of the final alkylimidazolium ILS were confirmed by ¹H-NMR, ¹³C-NMR, and ESI-IT MS, according with the spectral data below. The multiplicity of ¹H-NMR signals is given as before.

(a) *1-tetradecyl-3-(prop-2-enyl)imidazolium bromide*. White solid (0.3887 g, 45.2%); δ_H/ppm (400 MHz, CDCl₃) 10.45 (s, 1H), 7.63 (t, 1H, J = 1.6 Hz), 7.40 (t, 1H, J = 1.6 Hz), 5.44 (d, 2H, J = 2.6 Hz), 4.31 (t, 2H, J = 7.5 Hz), 2.72 (t, 1H, J = 2.6 Hz), 1.91(q, 2H, J = 7.4 Hz), 1.33-1.23 (m, 22H), 0.86 (t, 3H, J = 6.9 Hz); δ_C/ppm (100 MHz, CDCl₃) 137.1; 122.0; 121.9; 77.9; 74.3; 50.6; 40.1; 32.0; 30.3; 29.7-29.4; 26.4; 22.8; 14.2; (EI⁺) *m/z* calculated for C₂₀H₃₅N₂⁺: 303.28; found: 303.87 [M]⁺; 687.47 [2M+Br]⁺.

(b) *1-hexadecyl-3-(prop-2-enyl)imidazolium bromide*. White solid (0.634 g, 97%); δ_H/ppm (400 MHz, CDCl₃) 10.5 (s, 1H), 7.65 (s, 1H), 7.43 (s, 1H), 5.45 (d, 2H, J = 3.0 Hz), 4.31 (t, 2H, J = 7.5 Hz), 2.72 (t, 1H, J = 2.4 Hz), 1.90 (q, 2H, J = 7.1 Hz), 1.33-1.23 (m, 26H), 0.85 (t, 3H, J = 6.9 Hz); δ_C/ppm (100 MHz, CDCl₃) 137.1, 122.1, 122.0; 77.9, 74.3, 50.6, 40.1, 32.0, 30.3, 29.8-29.4, 29.1, 26.4, 22.8, 14.2; (EI⁺) *m/z* calculated for C₂₂H₃₉N₂⁺: 331.31, found 331.50 [M]⁺; 743.24 [2M+Br]⁺.

(iii) On-resin peptide sequence assembly. All peptide derivatives based on the amino acid sequence of the parent PP4 (amino acid sequence KTKS), and this reference peptide itself, were assembled by standard SPPS procedures using the Fmoc^tBu orthogonal protection scheme (49). The Fmoc-Rink-amide MBHA resin (100 to 200 mesh, 0.52 mmol/g; NovaBiochem) was used as solid support for the assembly of all peptides except for peptide C₁₆-KTKS-OH that was assembled on a preloaded Fmoc-Ser^t(Bu)-Wang resin (100 to 200 mesh, 0.69 mmol/g; NovaBiochem). In all cases, the commercial Fmoc-protected resin was first swelled in *N,N*-dimethylformamide (DMF; CARLO ERBA) for 30 min and next treated with piperidine (20%; MERCK) in DMF for 20 min at r.t., for removal of the Fmoc protecting group. After washing steps using DMF and DCM (3 × 10 mL), coupling of the desired amino acid residue was performed using a mixture of the Fmoc-protected amino acid (5 eq; Bachem), *O*-(benzotriazol-1-yl)-*N,N,N',N'*-tetramethyluronium hexafluorophosphate (HBTU, 5 eq; NovaBiochem), and *N*-ethyl-*N,N*-diisopropylamine (DIEA, 10 eq; VWR), which was added to the resin and kept at r.t. for 1 h, under stirring. The deprotection and coupling cycles were repeated under the same conditions until the full amino acid sequence was assembled and, whenever desired, the Fmoc-Lys(Boc)-OH (NovaBiochem) standard building block was replaced by its *ε*-azide analogue, Fmoc-Lys(N₃)-OH. For the synthesis of the *N*-terminally modified peptides, namely, 2-azidoethanoyl-KTKS (N₃-KTKS) and the reference palmitoyl

peptides C₁₆-KTTKS-NH₂ and C₁₆-KTTKS-OH, the same general procedure was adopted, with an additional sequence elongation step using, respectively, 2-azidoacetic (37.5 μ L, 0.5 mmol, 5 eq; Sigma-Aldrich) or palmitic (0.128 mg, 0.5 mmol, 5 eq; Sigma-Aldrich) acids instead of a Fmoc-protected amino acid.

(iv) On-resin “click” reaction (CuAAC). While still anchored to the resin, azide-modified peptides were further reacted with the relevant propargyl-ILs *via* CuAAC. To this end, a solution containing the relevant propargyl-IL (Pr-Melm) (20 mg, 0.1 mmol, 1 eq), Pr-C₁₆Im (53 mg, 0.12 mmol, 1.2 eq) or Pr-C₁₄Im (38.3 mg, 0.1 mmol, 1 eq), 2,6 lutidine (116 μ L, 1 mmol, 10 eq; Alfa Aesar), sodium L-ascorbate (19.8 mg, 0.1 mmol, 1 eq; Sigma-Aldrich), and DIEA (170 μ L, 1 mmol, 10 eq; VWR) in DMF (3 mL) was added to the desired azido-peptidyl resin, followed by addition of copper(I) bromide (14.3 mg, 0.1 mmol, 1 eq; Fluka) in ACN (1 mL; CARLO ERBA). The “click” reaction was allowed to proceed at r.t. under stirring for 24 h. After draining the resin, this was thoroughly washed with 0.1 M aqueous ethylenediaminetetraacetic acid (EDTA, 5 \times 10 mL; PanReac AppliChem) to ensure full removal of copper, followed by DMF (3 \times 10 mL) and DCM (3 \times 10 mL), to wash out all other unreacted materials and side products.

(v) Cleavage and purification of final peptides and their IL conjugates. Once fully assembled, the peptides were fully deprotected and released from the solid support through a 2h acidolysis using a cleavage cocktail containing 95% of TFA (VWR), 2.5% of triisopropylsilane (TIS; Alfa Aesar), and 2.5% of deionized water. The crude peptide material thus obtained was next purified by RP-HPLC on a Hitachi-Merck LaPrep Sigma system equipped with an LP3104 UV detector and an LP1200 pump, using an RP-C₁₈ column (250 \times 25 mm, 5 μ m pore size) and an elution gradient using 0.05% aqueous TFA as solvent A and acetonitrile (ACN) as solvent B. The pure peptide fractions were collected, pooled, and freeze-dried to afford the final peptide as a fluffy white solid.

(vi) Quantitation of final peptides and their IL conjugates. Peptide stock solutions were prepared at approximately 10 mg/mL in distilled water except for C₁₆-KTTKS-OH that was solubilized in DMSO. Accurate quantitation of the peptide solutions were quantitated by microvolume spectrophotometry at 205 nm, using a Thermo Scientific NanoDrop One system and quantitation method 31 that assumes an extinction coefficient ϵ_{205} of 31 mL \cdot mg⁻¹ \cdot cm⁻¹ (50). Exception was made for the reference peptide C₁₆-KTTKS-OH, which was quantified through amino acid analysis (AAA) due to its poor solubility in water, making it inadequate for NanoDrop. To this end, the peptide was hydrolyzed using 6 M aqueous hydrochloric acid containing phenol (10% vol/vol), for 24 h at 110°C. The hydrolysate was next evaporated to dryness and the residue dissolved in HPLC-grade water (500 μ L) containing α -aminobutyric acid as internal standard. The mixture thus obtained was then derivatized by the AccQ-Tag protocol from Waters using 6-aminoquinoyl-*N*-hydroxysuccinimidyl carbamate (51), and the resulting solution analyzed by HPLC (WATERS 600) with the UV-detector (WATERS 2487) set at 254 nm.

In vitro assays. (i) Antibacterial activity in standard conditions. The test conjugates and reference compounds were evaluated for their activity against three reference strains of Gram-negative bacteria, namely, *E. coli* (ATCC 25922), *Pseudomonas aeruginosa* (ATCC 27853), and *Klebsiella pneumoniae* (ATCC 13883), and the four following reference strains of Gram-positive bacteria, *Staphylococcus aureus* (ATCC 29213), *S. Epidermidis* (ATCC 14990), *E. faecalis* (ATCC 29212), and *Streptococcus pyogenes* (ATCC 19615). MIC values were assessed using the broth microdilution method in cation adjusted MHB2 - Sigma-Aldrich, except for *S. pyogenes* (a group A beta-hemolytic *Streptococcus*), where the medium was previously supplemented with lysed horse blood (Sigma-Aldrich) at 2.5% according to the CLSI guidelines (28). MBC values were also determined as previously reported (52). The two conjugates displaying higher antibacterial activity were further evaluated by determining their MIC against MDR clinical isolates of *K. pneumoniae* (KP010), *P. aeruginosa* (PA004), and *S. aureus* (SA007).

(ii) Antibacterial activity in simulated wound fluid. MIC values of the most active conjugates, C₁₆Im-KTTKS and KTKK(C₁₆Im)_S, were also determined in SWF against *S. aureus* (ATCC 29213). Briefly, the conjugates were dissolved in water and diluted in 0.02% aqueous acetic acid containing 0.4% of bovine serum albumin (BSA; Sigma-Aldrich) to final concentrations ranging from 1,280 to 1.25 μ g/mL. In parallel, SWF was prepared to a final composition of 50% fetal bovine serum (FBS; Sigma-Aldrich) and 50% peptone water (0.9% NaCl in 0.1% aqueous peptone; Sigma-Aldrich) (35). *S. aureus* was incubated (10⁵ CFU/mL) in either MHB or SWF in the presence of the test conjugates at concentrations between 128 and 0.125 μ g/mL, and bacterial growth assessed after 18 h of incubation at 37°C. MIC values were determined in triplicates and are a result of three independent experiments. MBC values were also determined by plating 10 μ L of the content of the first three wells where bacterial growth was not observed, followed by incubation in Tryptic Soy Agar (TSA; Sigma-Aldrich) for 24 h at 37°C.

(iii) Antifungal activity. The two conjugates with stronger antibacterial action, and relevant parent compounds and their mixture, were also tested for antifungal activity, using three reference strains of *Candida* spp., namely, *C. albicans* ATCC 90028, *C. glabrata* ATCC 90030, and *C. parapsilosis* ATCC 22019. MIC values were determined using a broth microdilution method in RPMI 1640, supplemented with glucose to a final concentration of 2% (RPMI 2% G), according to the EUCAST protocol (36).

(iv) Toxicity to human cells. HaCat and HFF-1 were seeded at 4 \times 10⁴ cell/mL in 96-well plate using in Dulbecco’s Modified Eagle Medium (DMEM; CLS) supplemented with 2% FBS (Biowest) and 1% of antibiotic/antimycotic solution (100 units/mL of penicillin, 10 mg/mL of streptomycin, and 0.25 mg/mL of amphotericin B, Sigma-Aldrich). The plate was incubated at 37°C in a 5% CO₂ atmosphere, and the cells allowed to grow until confluence was reached. Then, solutions of the test compounds in DMEM supplemented with 2% FBS, in a concentration range between 6.3 and 100 μ M, were added to the wells. After 24 h of incubation at 37°C in a 5% CO₂ atmosphere, the cell viability was assessed through the resazurin reduction assay. Briefly, the medium was removed and then 20 μ L of the alamarBlue Cell Viability Reagent (Resazurin sodium salt, Sigma-Aldrich) at 0.15 mg/mL in 100 μ L of Hank’s Balanced Salt Solution (HBSS; Sigma-Aldrich) were added to each well; the plate was next incubated for 2 h at 37°C in a 5% CO₂

atmosphere, after which fluorescence was read at 560/590 nm on a Flex Station 3 multi-mode microplate reader (Molecular Devices) (53). The IC₅₀ values were thus determined using the GraphPad Prism 9.0 software, by applying the equation log(inhibitor) versus response with variable slope (four parameters).

(v) Collagen production in human dermal fibroblasts. The amount of collagen produced by HDF was determined using the SIRCOL Kit Assay (Biocolor) according to the manufacturers' instructions (38). Briefly, the cells were seeded in 6-well plates, using DMEM supplemented with 10% FBS and 1% antibiotic/antimycotic solution. When confluence was achieved, DMEM supplemented with 2% of FBS and containing the test conjugates at 5 μM was added to the cell cultures, which were then incubated over 48 h at 37°C in a 5% CO₂ atmosphere. Medium was then removed, and quantitation of the newly formed collagen proceeded as follows: collagen was solubilized in cold 0.5 M aqueous acetic acid (Fisher Chemical) and concentrated overnight with deposition of a transparent pellet; after centrifugation, the supernatant was discarded and the pellet was labeled with the SIRCOL dye reagent; after removing the unbound dye with the acid-salt wash reagent, the collagen-bound dye was dissolved with the alkali reagent and absorbance was measured at 555 nm on Flex Station 3 multimode microplate reader. The collagen concentration was then determined by interpolation in a standard curve built by using the same quantitation method on standard solutions of rat collagen in 0.5 aqueous acetic acid.

Results were expressed as mean ± standard error of mean (SEM) values for collagen amount (% of control) and the statistical analysis was performed in GraphPad Prism 9.0.0 Software using T student, paired test, *P* values two-tailed with confidence interval of 95% (*, *P* < 0.05; **, *P* < 0.01).

ACKNOWLEDGMENTS

This work received financial support from National Funds (FCT, Fundação para a Ciência e Tecnologia) through project CIRCNA/BRB/0281/2019. FCT is also acknowledged for supporting the LAQV-REQUIMTE research unit (UIDB/50006/2020) and for the research contract of I.F. (SFRH/BPD/86173/2012). Thanks are also due to the Portuguese NMR network (RNRMN), for support to the Laboratory for Structural Elucidation (LAE) of the Materials Centre of the University of Porto (CEMUP).

We declare no conflicts of interest.

Conceptualization, C.T., R.F., P.Ga., M.C.L.M., P.Go.; investigation, A.G., L.J.B., I.F., L.A., C.M.; writing—original draft, A.G., L.J.B., I.F., C.M.; writing—review & editing, C.T., R.F., P.Ga., N.M., M.C.L.M., P.Go.; supervision, R.F., P.Ga., C.T., N.M., M.C.L.M., P.Go. All authors have read and agreed to the published version of the manuscript.

REFERENCES

- Leong HN, Kurup A, Tan MY, Kwa ALH, Liau KH, Wilcox MH. 2018. Management of complicated skin and soft tissue infections with a special focus on the role of newer antibiotics. *Infect Drug Resist* 11:1959–1974. <https://doi.org/10.2147/IDR.S172366>.
- Golan Y. 2019. Current treatment options for acute skin and skin-structure infections. *Clin Infect Dis* 68:S206–S212. <https://doi.org/10.1093/cid/ciz004>.
- Esposito S, Ascione T, Pagliano P. 2019. Management of bacterial skin and skin structure infections with polymicrobial etiology. *Expert Rev Anti Infect Ther* 17:17–25. <https://doi.org/10.1080/14787210.2019.1552518>.
- Kalan L, Loesche M, Hodkinson BP, Heilmann K, Ruthel G, Gardner SE, Grice EA. 2016. Redefining the chronic-wound microbiome: fungal communities are prevalent, dynamic, and associated with delayed healing. *mBio* 7:1–12. <https://doi.org/10.1128/mBio.01058-16>.
- Kalan L, Grice EA. 2018. Fungi in the wound microbiome. *Adv Wound Care (New Rochelle)* 7:247–255. <https://doi.org/10.1089/wound.2017.0756>.
- Beyene RT, Derryberry SL, Jr, Barbul A. 2020. The effect of comorbidities on wound healing. *Surg Clin North Am* 100:695–705. <https://doi.org/10.1016/j.suc.2020.05.002>.
- Gonzalez ACdO, Costa TF, Andrade ZA, Medrado ARAP. 2016. Wound healing - a literature review. *An Bras Dermatol* 91:614–620. <https://doi.org/10.1590/abd1806-4841.20164741>.
- Chattopadhyay S, Raines RT. 2014. Review collagen-based biomaterials for wound healing. *Biopolymers* 101:821–833. <https://doi.org/10.1002/bip.22486>.
- Banerjee P, Suguna L, Shanthi C. 2015. Wound healing activity of a collagen-derived cryptic peptide. *Amino Acids* 47:317–328. <https://doi.org/10.1007/s00726-014-1860-6>.
- Sato K, Asai TT, Jimi S. 2020. Collagen-derived di-peptide, prolylhydroxyproline (pro-hyp): a new low molecular weight growth-initiating factor for specific fibroblasts associated with wound healing. *Front Cell Dev Biol* 8. <https://doi.org/10.3389/fcell.2020.548975>.
- Sivaraman K, Shanthi C. 2018. Matrikines for therapeutic and biomedical applications. *Life Sci* 214:22–33. <https://doi.org/10.1016/j.lfs.2018.10.056>.
- Maquart FX, Bellon G, Pasco S, Monboisse JC. 2005. Matrikines in the regulation of extracellular matrix degradation. *Biochimie* 87:353–360. <https://doi.org/10.1016/j.biochi.2004.10.006>.
- Abu Samah NH, Heard CM. 2011. Topically applied KTTKS: a review. *Int J Cosmet Sci* 33:483–490. <https://doi.org/10.1111/j.1468-2494.2011.00657.x>.
- Katayama K, Armendariz-Borunda J, Raghov R, Kang AH, Seyer JM. 1993. A pentapeptide from type I procollagen promotes extracellular matrix production. *J Biol Chem* 268:9941–9944. [https://doi.org/10.1016/S0021-9258\(18\)82153-6](https://doi.org/10.1016/S0021-9258(18)82153-6).
- Aldag C, Nogueira Teixeira D, Leventhal PS. 2016. Skin rejuvenation using cosmetic products containing growth factors, cytokines, and matrikines: a review of the literature. *Clin Cosmet Invest Dermatol* 9:411–419. <https://doi.org/10.2147/CCID.S116158>.
- Robinson LR, Fitzgerald NC, Doughty DG, Dawes NC, Berge CA, Bissett DL. 2005. Topical palmitoyl pentapeptide provides improvement in photo-aged human facial skin. *Int J Cosmet Sci* 27:155–160. <https://doi.org/10.1111/j.1467-2494.2005.00261.x>.
- Gomes A, Bessa LJ, Fernandes I, Ferraz R, Mateus N, Gameiro P, Teixeira C, Gomes P. 2019. Turning a collagenesis-inducing peptide into a potent antibacterial and antibiofilm agent against multidrug-resistant gram-negative bacteria. *Front Microbiol* 10:1915–1911. <https://doi.org/10.3389/fmicb.2019.01915>.
- Gomes A, Bessa LJ, Correia P, Fernandes I, Ferraz R, Gameiro P, Teixeira C, Gomes P. 2020. “Clicking” an ionic liquid to a potent antimicrobial peptide: on the route towards improved stability. *Int J Mol Sci* 21:1–11.
- Egorova KS, Gordeev EG, Ananikov VP. 2017. Biological activity of ionic liquids and their application in pharmaceuticals and medicine. *Chem Rev* 117:7132–7189. <https://doi.org/10.1021/acs.chemrev.6b00562>.
- Reddy GKK, Nancharaiah YV. 2020. Alkylimidazolium ionic liquids as antifungal alternatives: antibiofilm activity against *Candida albicans* and underlying mechanism of action. *Front Microbiol* 11:730–730. <https://doi.org/10.3389/fmicb.2020.00730>.

21. Forero DO, Castro R, Gutierrez M, Gonzalez VD, Santos L, Ramirez D, Guzman L. 2018. Novel alkylimidazolium ionic liquids as an antibacterial alternative to pathogens of the skin and soft tissue infections. *Molecules* (Basel, Switzerland) 23:2354. <https://doi.org/10.3390/molecules23092354>.
22. Sidat Z, Marimuthu T, Kumar P, Du Toit LC, Kondiah PPD, Choonara YE, Pillay V. 2019. Ionic liquids as potential and synergistic permeation enhancers for transdermal drug delivery. *Pharmaceutics* 11:96. <https://doi.org/10.3390/pharmaceutics11020096>.
23. Zhang D, Wang H-J, Cui X-M, Wang C-X. 2016. Evaluations of imidazolium ionic liquids as novel skin permeation enhancers for drug transdermal delivery. *Pharm Dev Technol* 22:1–10.
24. Gomes A, Aguiar L, Ferraz R, Teixeira C, Gomes P. 2021. The emerging role of ionic liquid-based approaches for enhanced skin permeation of bioactive molecules: a snapshot of the past couple of years. *Int J Mol Sci* 22:11991. <https://doi.org/10.3390/ijms222111991>.
25. Zakrewsky M, Lovejoy KS, Kern TL, Miller TE, Le V, Nagy A, Goumas AM, Iyer RS, Del Sesto RE, Koppisch AT, Fox DT, Mitragotri S. 2014. Ionic liquids as a class of materials for transdermal delivery and pathogen neutralization. *Proc Natl Acad Sci U S A* 111:13313–13318. <https://doi.org/10.1073/pnas.1403995111>.
26. Colonna M, Berti C, Binassi E, Fiorini M, Sullalti S, Acquasanta F, Vannini M, Di Gioia D, Aloisio I, Karanam S, Brunelle DJ. 2012. Synthesis and characterization of imidazolium telechelic poly(butylene terephthalate) for antimicrobial applications. *React Funct Polym* 72:133–141. <https://doi.org/10.1016/j.reactfunctpolym.2011.12.003>.
27. Hu Q, Deng Y, Yuan Q, Ling Y, Tang H. 2014. Polypeptide ionic liquid: synthesis, characterization, and application in single-walled carbon nanotube dispersion. *J Polym Sci Part A: Polym Chem* 52:149–153. <https://doi.org/10.1002/pola.26991>.
28. Patel JB. 2012. Methods for dilution antimicrobial susceptibility tests for bacteria that grow aerobically; approved standard M7-A9. Clinical and Laboratory Standards Institute, Wayne, PA, USA.
29. Postleb F, Stefanik D, Seifert H, Giernoth R. 2013. BIONic liquids: imidazolium-based ionic liquids with antimicrobial activity. *Zeitschrift Für Naturforschung B* 68:1123–1128. <https://doi.org/10.5560/znb.2013-3150>.
30. Büttner H, Mack D, Rohde H. 2015. Structural basis of Staphylococcus epidermidis biofilm formation: mechanisms and molecular interactions. *Front Cell Infect Microbiol* 5:14. <https://doi.org/10.3389/fcimb.2015.00014>.
31. Sadeghpour Heravi F, Zakrzewski M, Vickery K, G Armstrong D, Hu H. 2019. Bacterial diversity of diabetic foot ulcers: current status and future perspectives. *J Clin Med* 8:1935. <https://doi.org/10.3390/jcm8111935>.
32. Walker MJ, Barnett TC, McArthur JD, Cole JN, Gillen CM, Henningham A, Sriprakash KS, Sanderson-Smith ML, Nizet V. 2014. Disease manifestations and pathogenic mechanisms of group A streptococcus. *Clin Microbiol Rev* 27:264–301. <https://doi.org/10.1128/CMR.00101-13>.
33. Pato C, Melo-Cristino J, Ramirez M, Friães A, Vaz T, Gião M, Ferreira R, Silva AC, Costa H, Silva MF, Afonso MA, Domingos A, Marrão G, Grossinho J, Lopes P, Lameirão A, Abreu G, Selaru A, Marques H, Tomaz M, Mota P, Ramos MH, Castro AP, Fonseca F, Canhoto N, Afonso T, Pina T, Peres H, Chantre O, Marques J, Marcelo C, Peres I, Lourenço I, Pinto M, Monteiro L, Lito LM, Toscano CA, Pessanha MRE, Díaz R, Ferreira S, Roxo IC, Castro AP, Ribeiro G, Tomé R, Pontes C, Boaventura L, Chaves C, Reis T, TPGftSoSI, et al. 2018. Streptococcus pyogenes causing skin and soft tissue infections are enriched in the recently emerged emm89 clade 3 and are not associated with abrogation of CovRS. *Front Microbiol* 9. <https://doi.org/10.3389/fmicb.2018.02372>.
34. Mulani MS, Kamble EE, Kumkar SN, Tawre MS, Pardesi KR. 2019. Emerging strategies to combat ESKAPE pathogens in the era of antimicrobial resistance: a review. *Front Microbiol* 10:539–539. <https://doi.org/10.3389/fmicb.2019.00539>.
35. Price BL, Lovering AM, Bowling FL, Dobson CB. 2016. Development of a novel collagen wound model to simulate the activity and distribution of antimicrobials in soft tissue during diabetic foot infection. *Antimicrob Agents Chemother* 60:6880–6889. <https://doi.org/10.1128/AAC.01064-16>.
36. EUCAST. 2020. The European Committee on Antimicrobial Susceptibility Testing.
37. Tałała U, Uściłowicz P, Bruzgo I, Surazyńska A, Zaręba I, Markowska A. 2019. The effects of a novel series of KTTKS analogues on cytotoxicity and proteolytic activity. *Molecules* 24:3698. <https://doi.org/10.3390/molecules24203698>.
38. Anonymous. 2021. Sircol collagen assay kit. <https://www.biocolor.co.uk/product/sircol-soluble-collagen-assay/>. Accessed September 22, 2021.
39. Iwai N, Nakayama K, Kitazume T. 2011. Antibacterial activities of imidazolium, pyrrolidinium and piperidinium salts. *Bioorg Med Chem Lett* 21:1728–1730. <https://doi.org/10.1016/j.bmcl.2011.01.081>.
40. Pendleton JN, Gilmore BF. 2015. The antimicrobial potential of ionic liquids: a source of chemical diversity for infection and biofilm control. *Int J Antimicrob Agents* 46:131–139. <https://doi.org/10.1016/j.ijantimicag.2015.02.016>.
41. Carson L, Chau PKW, Earle MJ, Gilea MA, Gilmore BF, Gorman SP, McCann MT, Seddon KR. 2009. Antibiofilm activities of 1-alkyl-3-methylimidazolium chloride ionic liquids. *Green Chem* 11:492–497. <https://doi.org/10.1039/b821842k>.
42. Agalave SG, Maujan SR, Pore VS. 2011. Click chemistry: 1,2,3-triazoles as pharmacophores. *Chem Asian J* 6:2696–2718. <https://doi.org/10.1002/asia.201100432>.
43. Breijyeh Z, Jubeh B, Karaman R. 2020. Resistance of Gram-negative bacteria to current antibacterial agents and approaches to resolve it. *Molecules* 25:1340. <https://doi.org/10.3390/molecules25061340>.
44. Wounds International. 2019. World Union of Wound Healing Societies (WUWHS) Consensus Document. Wound exudate: effective assessment and management. <https://www.wuwhs.org/wp-content/uploads/2020/09/exudate.pdf>.
45. Delaloye J, Calandra T. 2014. Invasive candidiasis as a cause of sepsis in the critically ill patient. *Virulence* 5:161–169. <https://doi.org/10.4161/viru.26187>.
46. Fatemi MH, Izadiyan P. 2011. Cytotoxicity estimation of ionic liquids based on their effective structural features. *Chemosphere* 84:553–563. <https://doi.org/10.1016/j.chemosphere.2011.04.021>.
47. Egorova KS, Seitkhalieva MM, Posvyatenko AV, Ananikov VP. 2015. An unexpected increase of toxicity of amino acid-containing ionic liquids. *Toxicol Res* 4:152–159. <https://doi.org/10.1039/C4TX00079J>.
48. Jones RR, Castelletto V, Connon CJ, Hamley IW. 2013. Collagen stimulating effect of peptide amphiphile C-16-KTTKS on human fibroblasts. *Mol Pharm* 10:1063–1069. <https://doi.org/10.1021/mp300549d>.
49. Behrendt R, White P, Offer J. 2016. Advances in Fmoc solid-phase peptide synthesis. *J Pept Sci* 22:4–27. <https://doi.org/10.1002/psc.2836>.
50. Loughrey S, Mannion J, Matlock B. 2021. Using the NanoDrop one to quantify protein and peptide preparations at 205 nm. Thermo Fisher Scientific, Wilmington, DE. <http://tools.thermofisher.com/content/sfs/brochures/ND-One-Protein-and-Peptide-r16-01-18.pdf>. Accessed August 20, 2021.
51. Waters Corporation. 2014. AccQ-Tag ultra derivatization kit. <https://www.waters.com/webassets/cms/support/docs/715001331.pdf>.
52. Gomes NM, Bessa LJ, Buttachon S, Costa PM, Buaruang J, Dethoup T, Silva AM, Kijjoa A. 2014. Antibacterial and antibiofilm activities of tryptoquivalines and meroditerpenes isolated from the marine-derived fungi Neosartorya paulistensis, N. laciniosa, N. tsunodae, and the soil fungi N. fischeri and N. siamensis. *Mar Drugs* 12:822–839. <https://doi.org/10.3390/md12020822>.
53. Riss TL, Moravec RA, Niles AL, Duellman S, Benink HA, Worzella TJ, Minor L. Cell Viability Assays. 2013. In Markossian S, Grossman A, Brimacombe K, Arkin M, Auld D, Austin CP, Baell J, Chung TDY, Coussens NP, Dahlin JL, Devanarayan V, Foley TL, Glicksman M, Hall MD, Haas JV, Hoare SRJ, Inglesse J, Iversen PW, Kales SC, Lal-Nag M, Li Z, McGee J, McManus O, Riss T, Saradjian P, Sittampalam GS, Tarselli M, Trask OJ, Jr, Wang Y, Weidner JR, Wildey MJ, Wilson K, Xia M, Xu X (eds), Assay Guidance Manual [Internet] May 1 [updated 2016 Jul 1]. PMID: 23805433. Eli Lilly & Company and the National Center for Advancing Translational Sciences, Bethesda MD.